Distributionally Robust Resilience Assessment of Power Systems with Offshore Wind Farms

1st Debin Zeng, 2nd Tianyang Zhao
Energy and Electric Research Center
Jinan University
Zhu Hai, China
dbzeng@stu2021.jnu.edu.cn

3rd Cheng Qian
Transmission Planning Consultant
Burns & McDonnell
Houston, Texas, United States
cqian@burnsmcd.com

4rd Jun Guo
State Key Laboratory of Disaster Prevention and Reduction for Power Grid Transmission and Distribution Equipment
Changsha, Hunan, China
332413817@qq.com

2022 IEEE/IAS Industrial and Commercial Power System Asia (I&CPS Asia) | 978-1-6654-5066-9/22/$31.00 ©2022 IEEE | DOI: 10.1109/ICPSAsia55496.2022.9949784

***Abstract*—More and more offshore wind farms (OWFs) are integrated into the power system to achieve sustainable energy development. Extreme events such as hurricanes damage transmission lines and affect OWFs power output. Considering the uncertain nature of hurricane evaluation stages, a novel jointed data and model-driven distributionally robust ambiguity set is formulated to quantify the impacts of hurricanes on power systems with OWFs. A Monte-Carlo simulation based assessment method is adopted to assess the resilience of power systems under nominal PDFs. The distributionally robust conditional value at risk (DRO-CVaR) is proposed to quantify the resilience of power systems with OWFs under total variation distance-based ambiguity density function. Simulations are performed on a modified IEEE RTS-24 system under the Kenta hurricane. The results indicate that the resilience of power systems towards hurricanes under distributionally robust ambiguities can be captured by nodal reliability level.**

***Index Terms*—Hurricane, offshore wind farms, distributionally robust, resilience assessment, conditional value at risk**

I. Introduction

The rapid development and integration of offshore wind farms (OWFs) help reach carbon emission reduction targets, but increase the susceptibility of power systems to extreme weather in the meantime. The temporal and spatial evolution of extreme weather events (EWEs), e.g., hurricanes, may damage transmission assets and change the output pattern of OWFs, threatening power system resilience. Resilience assessment is always the first step to mitigating these adverse impacts. Furthermore, before hurricane landfalls, features of hurricanes, such as hurricane paths and central pressures, were strongly uncertain in nature. Such uncertainties make the resilience assessment of power systems with OWFs challenging.

Research on classic power system resilience assessment mainly focuses on the modeling of extreme events, e.g., hurricanes [1]–[4]. Hurricanes are high-speed moving cyclones that produce strong winds and heavy rainfall within a certain spatial range. There are two wind field models [5] for tropical cyclones like hurricanes: one is a mesoscale atmospheric numerical model; the other is a parametric model of scenario-based statistical methods. Numerical models are still not enough to accurately estimate wind field strength and phase changes, while parametric models [6]–[9] can simulate high-speed wind fields in a specific area by using physical parameters extracted from historical data as input. The parametric models have a simple mathematical form and strong operability, so that is widely used in practical research works. Hurricane paths are often considered deterministic in power system resilience assessment studies. In reality, however, hurricane paths are uncertain and challenging to predict. The impact of hurricanes with uncertain tracks on the power output of OWFs has not yet received attention.

For any given hurricane information, tremendous research works have been conducted for the impact of extreme events on the power transmission equipment and OWFs [10]–[14], e.g., transmission lines, the power output, and the components of OWFs. Model-based and data-driven models are established on overhead lines [4] to quantify the impact of hurricanes on the towers and conductors of power transmission lines. For OWFs, the focus is on the failure model of wind turbine components and high wind speed shutdown events [15]–[17]. In the study of power system reliability modeling, the failure of submarine cables also has been modeled [18]. The above models have contributed to system resilience, but there is few research effort directly on the resilience assessment of the system under the combination of factors caused by hurricanes.

Several research efforts have been proposed to model the response of power systems under uncertain transmission equipment failures [19]–[21]. To ensure power systems are capable of withstanding multiple component failures, the power industry has revised the classic N-1 criterion and required power systems to withstand simultaneous failure of multiple components, i.e., N-k contingency criterion. Another contingency criterion, called N-1-1, represented by two consecutively isolated components, has also received extensive attention. Due to the correlation between components, the failure of one component may lead to the failure of other components, and consequently, the chain reaction between components may eventually lead to the collapse of the system. The power system has established various probabilistic models for the aforementioned contingency events, but for a specific accidental event such as a hurricane, it is necessary to rediscover,

This paper is supported by State Key Laboratory of Disaster Prevention and Reduction for Power Grid Transmission and Distribution Equipment.

understand and study the power system of cascading failures with uncertain offshore wind power output.

Regardless of prior research efforts, errors in hurricane track prediction information have not been integrated in the previous models. The wind fields induced by hurricanes are affected by the hurricanes' tracks and topography. Different hurricane paths result in different wind speeds at the locations of power substations, leading to different component failure probabilities. Different hurricane paths result in distinct combinations of transmission equipment failures. A data-driven distributionally robust ambiguity set is proposed to depict the probabilistic combinations of transmission equipment, e.g., submarine cables, and OWFs power output, which allows the probability of hurricane events (paths) to be unknown and ambiguous. This ambiguity set is used as the input of the resilience assessment model, which can better reflect the influence of the real hurricane trajectory change on the risk of the power system. The spatial-temporal distribution of transmission line failures, power supply reliability, and the improvement of the adequacy of offshore wind power are exposed by calculating the DRO-CVaR of resilience indices.

With this in mind, this paper proposes a distributionally robust resilience assessment model to more effectively quantify the resilience of power systems with OWFs under uncertain hurricane paths. Submarine cables are considered in the transmission line failure model. The set of uncertain hurricane paths is constructed as a jointed data and model-driven distributionally robust ambiguity set, which quantifies the impact of hurricanes on the systems. The Monte Carlo method is used to simulate hurricane paths and system states. A resilience indices system based on the calculation of DRO-CVaR is proposed to provide guidance for measuring the resilience of power systems with offshore wind farms under hurricanes. The DRO-CVaR of power load shedding and wind power curtailment is used to describe the power supply reliability level of the system, and the effect of the proposed distributionally robust resilience assessment model is verified by comparing with traditional expected energy not supplied (EENS) which is also the counterpart of power load shedding.

The rest of the paper is organized as follows: 1) A distributionally robust model for assessing the resilience of power systems with OWFs is developed in section II. 2) The DRO-CVaR of load shedding and wind power curtailment is proposed in section III, as the resilience indices for measuring the risk level of the system under hurricanes. 4) Four case studies are designed in section IV. 5) The conclusion is outlined at the end.

II. Resilience Models of Power Systems with Offshore Wind Farms

In this section, a distributionally robust ambiguity set for hurricane tracks, OWFs power output, and transmission line failures are formulated as the response of power equipment under hurricanes. The uncertain hurricane translation speed, forward direction, and relative speed are depicted by a data-driven approach. Under uncertain hurricane models, the OWFs power output and transmission line model are formulated as stochastic models. A jointed data and model-driven ambiguity set is formulated with discrete support using total variation distance.

A. Uncertain Hurricane Model

As the parametric models can generate hurricanes with arbitrary paths in a specific area, in this paper an ambiguity set of hurricane events needs to be established, so a scenario-based empirical model [9] is used to simulate a set of hurricane events. According to the random prediction information [22], the longitude and latitude of hurricane generation follow the normal distribution of $\mathcal{N}(27.44, 0.90)$ and $\mathcal{N}(86.34, 3.65)$, the translation speed follows the log-normal distribution with parameters $(1.73, 0.34)$, and the central pressure The difference follows a log-normal distribution with parameters $(3.80, 0.11)$, and the direction follows an $\mathcal{N}(0, 4)$ normal distribution.

After the hurricane is generated before landfall, it moves onto the sea and intensifies. After landfall, the intensity of the hurricane gradually attenuates and disappears. Using the empirical trajectory model, the forward speed, the forward direction, and the intensity (central pressure difference) of the hurricane can be obtained as follow:

$$\begin{aligned}\Delta \ln c = {} & a_1(t) + a_2(t)\psi(t) + a_3(t)\lambda(t) \\ & + a_4(t)\ln c(t) + a_5(t)\theta(t) + \varepsilon_c\end{aligned} \tag{1}$$

$$\begin{aligned}\Delta\theta = {} & b_1(t) + b_2(t)\psi(t) + b_3(t)\lambda(t) + b_4(t)c(t) \\ & + b_5(t)\theta(t) + b_6(t)\theta(t-\Delta t) + \varepsilon_\theta\end{aligned} \tag{2}$$

$$\begin{aligned}\ln I(t+\Delta t) = {} & d_1(t) + d_2(t)\ln I(t) + d_3(t)\ln I(t-\Delta t) \\ & + d_4(t)\ln I(t-2\Delta t) + d_5(t)T_s(t) \\ & + d_6(t)\left(T_s(t+\Delta t) - T_s(t)\right) + \varepsilon_I\end{aligned} \tag{3}$$

where $c(t)$ is the hurricane translation speed. $\theta(t)$ is hurricane forward direction. $I(t)$ is the relative strength which is described as the central pressure difference $\Delta P(t)$. Δt is the time step length[1]. It should be noted that the relative intensity of hurricanes increases offshore [23] and weakens on land [24].

The power component failure factors under hurricanes are strong winds and heavy rain. Using the wind field model established by [24], the gradient wind speed at r km from the hurricane center is given as follows:

$$V\left(r\left(t\right), t, h_d\right) = G_\tau V_G\left(r\left(t\right), t\right)\left(\frac{h_d}{h_G}\right)^\alpha \tag{4}$$

where $V\left(r\left(t\right), t, h_d\right)$ is the 3-second, 10-meter wind speed at the component location. G_τ is the gust factor. $V_G\left(r\left(t\right), t\right)$ is the gradient wind speed at radius r km to the hurricane center. $h_d = 10$ m. h_G is the gradient height.

[1] Δt is set in accordance with the power system simulation in Subsection II.E.

B. Offshore Wind Farms Model

The OWFs power output is the combination of a set of wind turbines. For each wind farm, its output under given wind speed is shown as follows:

$$p_w^t = \begin{cases} 0, & v \le V_{cut-in}, v \ge V_{cut-out} \\ c_{wt} n_{wt} v^2, & V_{cut-in} \le v \le V_{rated} \\ n_{wt} P_{rated}^{wt} & V_{rated} \le v \le V_{cut-out} \end{cases} \tag{5}$$

where $p_{e,w}^t$ (MW) is power output of wind farm which composed n_{wt} wind turbines. n_{wt} is number of wind turbines within each wind farm. v (m/s) is equivalent 10 minute average wind speed at the wind turbine. V_{cut-in}, $V_{cut-out}$, V_{rated}, and P_{rated}^{wt} are cut-in wind speed, cut-out wind speed, rated wind speed, and rated power of wind turbine, respectively. c_{wt} is the production factor.

C. Transmission Line Failure Model

The transmission lines, including both overhead lines and submarine cables, are affected by the strong wind and rainfall inducted by hurricanes. In this paper, the submarine cables are used to interconnect OWFs and the onshore power system.

1) Failure Model of Submarine Cables: Submarine cables are elements that connect OWFs with onshore power systems. The failure factors mainly consider insulation aging, joint failures, earthquakes, and hurricanes. The failure rate and repair rate for a specific type of submarine cable are functions of the length L, absolute temperature T, and electric field intensity E of the submarine cable [25]. The differential equation of the two-state Markov process is as follows:

$$\begin{cases} \frac{dP_0(L,T,E,t)}{dt} = -\lambda(L,T,E)P_0(t) + \mu(L,T,E)P_1(t) \\ \frac{dP_1(L,T,E,t)}{dt} = \lambda(L,T,E)P_0(t) - \mu(L,T,E)P_1(t) \end{cases} \tag{6}$$

where $P_0(t)$ and $P_1(t)$ are the probabilities of a submarine cable operating and outage at time t, respectively. $\lambda(L,T,E)$ and $\mu(L,T,E)$ are the failure rate and repair rate, respectively. The static failure probability of the submarine cable can be calculated by setting both sides of the above equations to zero.

2) Failure Model of Overhead Lines: The overhead lines are composed of towers and conductors. The main influence factors of the hurricane on the towers of overhead lines are strong wind and rainfall. The impact of rainfall is introduced into the equivalent wind speed, as reference [26], as follows:

$$\begin{aligned} \mathcal{V}_{\text{tw},k}^{*t} =& \mathcal{V}_{\text{tw},k}^t + a_{\text{tw}} (Rf_{\text{tw},k}^t)^{b_{\text{tw}}} \exp(c_{\text{tw}} \mathcal{V}_{\text{tw},k}^t) \\ & - d_{\text{tw}} \exp(e_{\text{tw}} \mathcal{V}_{\text{tw},k}^t), \ \forall t \in \mathcal{T}, k \in \mathcal{E}_{\text{tw}} \end{aligned} \tag{7}$$

where $\mathcal{V}_{\text{tw},k}^{*t}$ (m·s^{-1}) is the equivalent wind speed. $\mathcal{V}_{\text{tw},k}^t$ (m·s^{-1}) is the 3-second, 10-meter wind speed at the location of tower k. $Rf_{\text{tw},k}^t$ (mm·h^{-1}) is the rainfall rate at the tower site. a_{tw}, b_{tw}, c_{tw}, d_{tw} and e_{tw} are constants. $\mathcal{E}_{\text{tw}}$ is the set of transmission towers.

The log-normal fragility curve [27] can be used to describe the failure probability distribution of tower k, as follows:

$$\pi_{\text{tw},k}^t = \frac{1}{\sqrt{2\pi}\alpha_{\text{tw},k}} \int_{-\infty}^{x_{\text{tw},k}^t} \exp\left(\frac{-(\tau - \mu_{\text{tw},k}^t)^2}{2(\alpha_{\text{tw},k})^2} \right) d\tau, \quad \forall t \in \mathcal{T}, k \in \mathcal{E}_{\text{tw}} \tag{8}$$

where $x_{\text{tw},k}^t = \ln \mathcal{V}_{\text{tw},k}^{*t}$. $\mu_{\text{tw},k}$ and $\sigma_{\text{tw},k}$ are the logarithmic mean and standard deviation of wind attacking angle, respectively.

Hurricanes have the same impact on conductors as towers. The regression model has been proposed in [28]. The conductor of overhead lines can be divided into several segments of equal length, each of which has the same rainfall rate [4]. The time-varying failure rate of each conductor segment is given as follows:

$$\lambda_{\text{cs},k}^t = L_{\text{cs},k} \exp\left(\frac{a_{\text{cs},k} \mathcal{V}_{\text{cs},k}^t}{\mathcal{V}_{\text{dcs},k}} + \frac{b_{\text{cs},k} Rf_{\text{cs},k}^t}{Rf_{\text{dcs},k}} + c_{\text{cs},k} \right), \quad \forall t \in \mathcal{T}, k \in \mathcal{E}_{\text{cs}} \tag{9}$$

where $L_{\text{cs},k}$ (km) is the segment length. $\mathcal{V}_{\text{cs},k}^t$ (m·s^{-1}) and $Rf_{\text{cs},k}^t$ (mm·h^{-1}) are the wind speed and rainfall rate at the location of segment k, respectively. $\mathcal{V}_{\text{dcs},k}$ (m·s^{-1}) and $Rf_{\text{dcs},k}$ (mm·h^{-1}) are the design value of wind speed and rainfall rate for segment k, respectively. $a_{\text{cs},k}$, $b_{\text{cs},k}$, and $c_{\text{cs},k}$ are parameters derived from historical data. $\mathcal{E}_{\text{cs}}$ is the set of transmission conductor segments.

According to discrete-time Markov process [29], the failure probability $\pi_{\text{cs},k}^t$ of segment k is calculated as follows:

$$\pi_{\text{cs},k}^t = (1 - \pi_{\text{cs},k}^{t\text{-}1})(1 - \exp(-\lambda_{\text{cs},k}^t t)) + \pi_{\text{cs},k}^{t\text{-}1}, \quad \forall t \in \mathcal{T}, k \in \mathcal{E}_{\text{cs}} \tag{10}$$

In the hurricane process, tower and conductor segment failures are assumed to be independent of each other. The status of an overhead line is determined by the status of the individual component. In this paper, the forced transmission line outage caused by occasional factors is also considered. The failure probability of an overhead line is divided into two parts, which can be obtained from the series theorem and the superposition theorem, as follows:

$$\begin{aligned} P_l^t = & \left(\frac{t_f}{t_f + t_s} \right) I_n + \\ & \left[1 - \prod_{i=1}^{\mathcal{E}_{\text{cs}}} \left(1 - \pi_{\text{tw},k}^t(t) \right) \prod_{j=1}^{\mathcal{E}_{\text{cs}}} \left(1 - \pi_{\text{cs},k}^t(t) \right) \right] I_h \end{aligned} \tag{11}$$

where P_l is the failure probability of transmission line l in time slot t. I_f and I_t denote the binary variables of no hurricane and hurricane, respectively.

D. Ambiguity Set under Uncertain Hurricanes

Affected by topography and so on, the translation speed and direction of the hurricane will deviate from the original prediction, resulting in inaccurate wind farm output and time-varying failure probability in Eq.(1) - Eq.(4). The Monte Carlo

method is used to simulate an ambiguity set of hurricane paths. Then the scenarios containing the wind farm output and transmission line status under uncertain hurricane paths can be obtained.

The empirical probability density $\{\omega_{1,0}, \omega_{2,0}, \cdots, \omega_{s,0},\}$ which denotes Ψ_0 of the set Ω_S containing S hurricane path scenarios is obtained using methods such as nonparametric estimation [30]. Since the probability density Ψ_0 is uncertain, the ambiguity set U_S is constructed based on the L1 distance, as follow:

$$U_S = \left\{ \psi : \sum_{s=1}^{S} |\omega_{s,0} - \omega_s| \leq \tau_{\mathrm{DRO}} \right\} \tag{12}$$

where Ψ is the discrete probability density function supported by $\{\omega_1, \omega_2, \cdots, \omega_s,\}$,namely Ω_S. τ_{DRO} is the preset threshold. Each scenario s in U_S contains hurricane information the date, time t, central pressure difference $\Delta P(t)$, translation speed $c(t)$ and forward direction $\theta(t)$, etc.

E. Power System Operation Model with Offshore Wind Farms

OWFs make up wind farms that are connected to the onshore power system via submarine cables. The onshore wind farm is directly connected to the bus. The technical constraints of generators, transmission lines, power balance, and reserve requirements are formulated as follows:

$$P_g^t - R_g^t \leq p_g^t \leq P_g^t + R_g^t, \forall t \in \mathcal{T}, g \in \mathcal{G} \tag{12}$$

$$-\mathrm{R}_g^{60\text{-}} \Delta t \leq p_g^t - p_g^{t-1} \leq \mathrm{R}_g^{60+} \Delta t, \forall t \in \mathcal{T}, g \in \mathcal{G} \tag{13}$$

$$\begin{aligned} (I_k - 1) M \leq p_k^t - B_k \left(\gamma_k^{+,t} - \gamma_k^{-,t}\right) \\ \leq (1 - I_k) M, \ \forall t \in \mathcal{T}, k \in \mathcal{E}_{\mathrm{e}} \end{aligned} \tag{14}$$

$$-I_k P_k^{\max} \leq p_k^t \leq I_k P_k^{\max}, \ \forall t \in \mathcal{T}, k \in \mathcal{E}_{\mathrm{e}} \tag{15}$$

$$P_{\mathrm{d},j}^t \geq p_{\mathrm{ls},j}^t \geq 0, \ \forall t \in \mathcal{T}, j \in \mathcal{D} \tag{16}$$

$$I_w P_{W,w}^t \geq p_{\mathrm{wc},w}^t \geq 0, \ \forall t \in \mathcal{T}, j \in \mathcal{N}_{\mathrm{w}} \tag{17}$$

$$\begin{aligned} \sum_{w \in \mathcal{W}} P_w^t - \sum_{w \in \mathcal{W}} p_{wc,w}^t + \sum_{g \in \mathcal{G}_j} p_g^t + \sum_{k \in \delta_j^+} p_k^t - \sum_{k \in \delta_j^-} p_k^t = \\ P_{\mathrm{d},j}^t - p_{\mathrm{ls},j}^t, \ \forall t \in \mathcal{T}, j \in \mathcal{D} \end{aligned} \tag{18}$$

where $\mathcal{T}$ denotes the assessment horizon and divided into equal time intervals with a length of Δt = 1 h. $\mathcal{G}$, $\mathcal{E}_{\mathrm{e}}$, $\mathcal{D}$, $\mathcal{N}_{\mathrm{w}}$ are the set of generators,the set of transmission lines, the set of power buses, the set of wind farms, respectively. p_g^t, R_g^t, R_g^{60} are the generator power output (MW), the reserve capacity of unit g and the maximum 60-min ramp-up or ramp-down rate of unit g, respectively. B_k (S), M, p_k^t (MW), $\gamma_k^{+,t}$ (°), $\gamma_k^{-,t}$ (°), I_k^t, P_k^{max} are the reciprocal of reactance of branch k, a large number, the active power flow on branch k, the bus angle at the from and to bus of branch k, the operating status of branch k (1 for on-line, 0 for otherwise), and the rate of branch k, respectively. $P_{d,j}^t$ (MW), $p_{ls,j}^t$ (MW) are the load forecast and load shedding at bus j during time slot t. P_w^t, $p_{wc,w}^t$, I_w are the power output of wind farm w during time slot t, the wind power curtailment of wind farm w during time slot t and the operating status of submarine cable w, respectively.

Eq.(12)-Eq.(13) are the power capacity limitation with reserves. Eq.(14)-Eq.(15) are the power transmitted on each line and its power limit, respectively. Eq.(16)-Eq.(17) are the amount of load shedding in each load bus and the amount of wind power curtailment in each wind farm, respectively. Eq.(18) is the power balance of each bus, together with wind power curtailment.

III. Resilience Indices for Power Systems with Offshore Wind Farms under Hurricanes

In this section, a comprehensive resilience indices for power systems with OWFs under hurricanes is proposed, which is shown in Tab I. The resilience indices are divided into two types: operational indices and economic indices, which from the perspective of elements of the systems affected by hurricanes such as power transmission, power generation, and power demand. It should be noted that economic indices are cost quantifications of operational indices.

A. Operational Indices

The operational indices can be classified into two levels. The first-level operational indices, the infrastructure damage risk can be summarized into four second-level indices: the expected number of towers, conductors, and transmission lines(including submarine cables) damaged and the DRO-CVaR of transmission assets damaged. The flooding has not been considered in this paper, and the underground cable damage is not included in the resilience indices. The expected number of transmission lines damaged and the DRO-CVaR of the number of transmission lines damaged formulas are given here as follows:

$$\mathbb{E}\left(N_l\right) = \sum_{s \in S} \pi_s \sum_{\omega \in \Omega_s} \pi_\omega \sum_{t \in T} n_{1,s,\omega}^t \tag{19}$$

$$\begin{aligned} &\mathrm{CVaR}_{\mathrm{DRO},\beta}\left(N_1\right) = \\ &\max_{(S,\pi_s),(\Omega_s,\pi_\omega) \in \mathbb{P}} \left(\underset{\beta, s \sim (S,\pi_s), \omega \sim (\Omega_s,\pi_\omega)}{\mathrm{CVaR}} \left(\sum_{t \in T} n_{1,s,\omega}^t \right) \right) \end{aligned} \tag{20}$$

where N_l is the total number of damaged transmission lines. $n_{l,s,\omega}^t$ is the number of transmission lines damaged under the scenario ω of hurricane path s during the time slot t. S is the number of forecast hurricane paths. Ω_s is the number of possible combinations of transmission line failure events under hurricane track s. π_s is the probability of hurricane track s. π_ω is the probability of scenario ω. β is the confidence level of 95%, and $\mathbb{P}$ is the distribution robust ambiguity set, such as the total variation distance ambiguity set.

The load shedding risk can be summarized into five second-level operational indices. Eq.(21) - Eq.(25) are the maximum load shedding at each load bus, the expected load shedding at each load bus, the maximum load shedding, the expected load shedding, i.e., EENS, and the DRO-CVaR of expected load

shedding at each load bus, respectively. The formulas are as follows:

$$p_{1s,d,\max} = \max_{s\in S,\omega\in\Omega_s,t\in T} p^t_{1s,d,s,\omega} \tag{21}$$

$$\mathbb{E}\left(p_{1s,d}\right) = \sum_{s\in S}\pi_s \sum_{\omega\in\Omega_s}\pi_\omega \sum_{t\in T} p^t_{1s,d,s,\omega} \tag{22}$$

$$p_{1s,\max} = \max_{s\in S,\omega\in\Omega_s,t\in T,d\in\mathcal{D}} p^t_{1s,d,s,\omega} \tag{23}$$

$$\mathbb{E}\left(p_{1s}\right) = \sum_{s\in S}\pi_s \sum_{\omega\in\Omega_s}\pi_\omega \sum_{d\in D}\sum_{t\in T} p^t_{1s,d,s,\omega} \tag{24}$$

$$\mathrm{CVaR}_{\mathrm{DRO},\beta}\left(p_{1s,d}\right) = \max_{(S,\pi_s),(\Omega_s,\pi_\omega)\in\mathbb{P}} \left(\underset{\beta,s\sim(S,\pi_s),\omega\sim(\Omega_s,\pi_\omega)}{\mathrm{CVaR}} \left(\sum_{t\in T} p^t_{1s,d,s,\omega} \right) \right) \tag{25}$$

where $\mathcal{D}$ is the set of power bus. $p^t_{ls,d,\omega,s}$ is the load shedding at bus d under the scenario ω of hurricane path s during time slot t. Similarly, wind power curtailment risk can also be divided into five second-level operational indices: the maximum wind power curtailment at each wind farm, the expected wind power curtailment at each wind farm, the maximum wind power curtailment, the expected wind power curtailment, and the DRO-CVaR of expected wind power curtailment at each wind farm. The formula refers to Eq.(21) - Eq.(25).

B. Economic Indices

The economic indices shown in Tab I can be obtained by multiplying various operational indices by economic coefficients.

TABLE I
RESILIENCE INDICES OF POWER SYSTEMS WITH OFFSHORE WIND FARMS UNDER HURRICANES

Resilience Indices	Affected Elements	First-level indices	Second-level indices
Operational Indices	Transmission (Transmission Line)	The infrastructure damaged risk	The expected number of towers damaged
			The expected number of conductors damaged
			The expected number of transmission lines damaged
			The distributionally robust CVaR of transmission assets damaged
	Power Generation (Wind Farm)	Wind power curtailment risk	The maximum wind power curtailment at each wind farm
			The expected of wind power curtailment at each wind farm
			The maximum wind power curtailment
			The expected wind power curtailment
			The distributionally robust CVaR of EWPC at each wind farm
	Power demand (Load bus)	Load shedding risk	The maximum load shedding at each load bus
			The expected of load shedding at each load bus
			The maximum load shedding
			The expected load shedding
			The distributionally robust CVaR of expected load shedding at each load bus
Economic Indices	Transmission (Transmission Line)	The infrastructure damage cost risk	The maximum repair and replacement cost of the tower/conductor/transmission line
			The expected repair and replacement cost of the tower/conductor/transmission line
			DRO-CVaR of transmission assets repair and replacement cost
	Power Generation (Wind Farm)	Wind power curtailment cost risk	The maximum cost of wind power curtailment
			The expected cost of wind power curtailment
			DRO-CVaR of wind power curtailment cost
	Power demand (Load bus)	Load shedding cost risk	The maximum cost of load shedding
			The expected cost of load shedding
			DRO-CVaR of load shedding cost

IV. RESILIENCE ASSESSMENT METHOD FOR POWER SYSTEMS WITH OFFSHORE WIND FARMS UNDER HURRICANES

In this section, the distributionally robust resilience assessment method is introduced, based on integrating the models and the resilience indices built-in Section II and Section III. The assessment procedure shown in Fig. 1 is described in detail as follows:

Step 1: Data acquisition

Step 1.1: System data, including the power system topology; load forecast; system operation constraints; the number of wind turbines and wind farms; wind farm power output and the cut-in and cut-out wind speed, etc. Structural features and value of exposed components such as design collapse, wind speed, rainfall, component cost, etc.

Step 1.2: Geographical data, including the geographic location of the exposed elements and the topographical features of the geographic location, these data are used to calculate the wind speed at the component site and wind farm site.

Step 1.3: Hurricane event data: the prediction time-varying hurricane center location (longitude, latitude), translation speed, central pressure deficiency, and coefficients needed in the hurricane wind field model; the ambiguity set U_S of possible hurricane paths.

Step 2: The hurricane path, hurricane location(longitude, latitude), date, time, relative intensity, direction, moving speed, etc., is sampled from the hurricane path ambiguity set S and according to the probability density of the hurricane path ω_s.

Step 3: Based on the selected hurricane event information, calculate the failure probability of transmission line components and the wind speed and wind power output of wind turbines in the wind farm.

Step 4: The transmission line status is simulated by the Monte Carlo method [4].

Step 5: Resilience indices calculation. During the entire analysis time horizon $\mathcal{T}$, the system status is checked for failure components. If not, start a new round of component failure simulation. Calculate and update infrastructure indices if any components fail. Then, the optimal power flow calculation is performed to determine the load shedding and wind power curtailment in the time horizon $\mathcal{T}$. Finally, each simulation's infrastructure damage, load shedding, and wind power curtailment are obtained, and their DRO-CVaR is calculated to measure the system risk level.

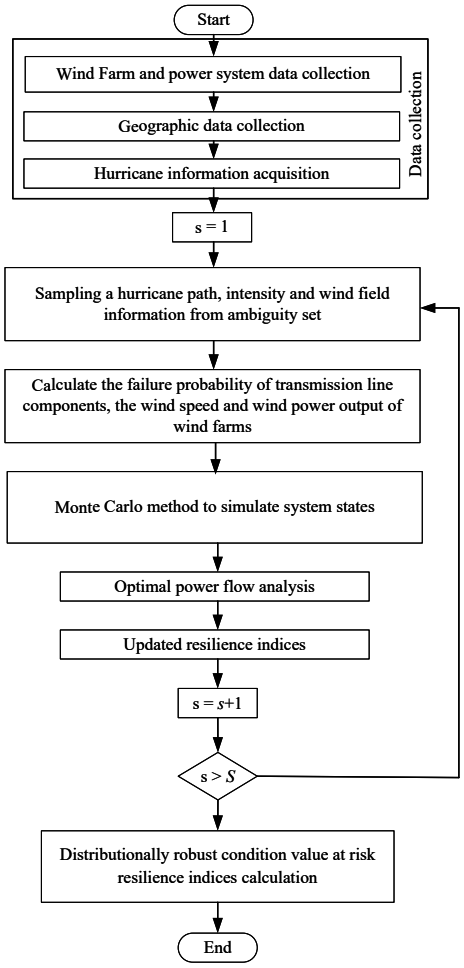

Fig. 1. Flowchart of power system resilience assessment under hurricanes.

V. Case Studies

A. Case Description

In this study, the IEEE RTS-24 system is projected to a region of 140 km * 200 km, as shown in Fig. 2. According to the hurricane resistance design requirements of transmission lines and the direction of coastal lines, this region is divided into ten regions. The system consists of 33 generators, 34 transmission lines (two submarine cables), and 6 transformers. The installed capacity of the system is 3402.5 MW. The peak load is 2830 MW and the wind power permeability will be designed at 11.85%.

1) Wind Farm Layout: Two onshore and two OWFs are connected to bus 23, 24 and bus 2, 7, respectively. Each wind farm is comprised of 24 wind turbines, and the total installed capacity is 100.8 MW. The parameters of wind turbines seen in section II.B. It should be noted that the location of the offshore wind farms is designed to be 17 km away from the coastline.

2) Test Cases: To illustrate the validity of the proposed assessment model, four comparative cases are designed to illustrate the impact of hurricanes and wind power on power

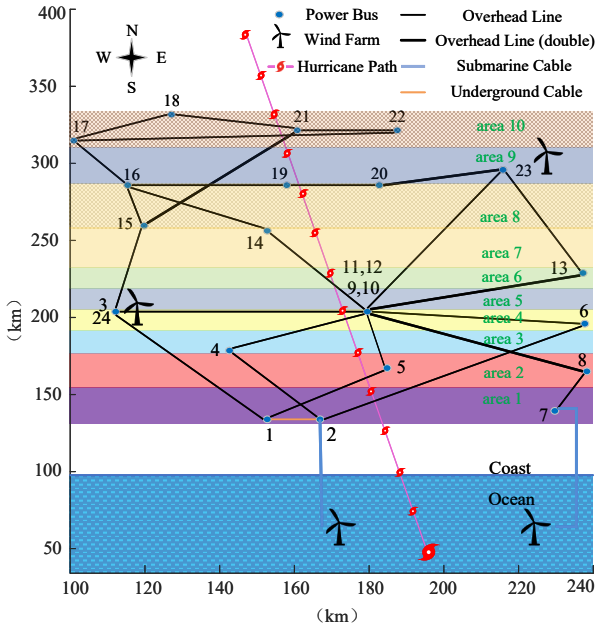

Fig. 2. Single line diagram of IEEE RTS-24 under a hurricane.

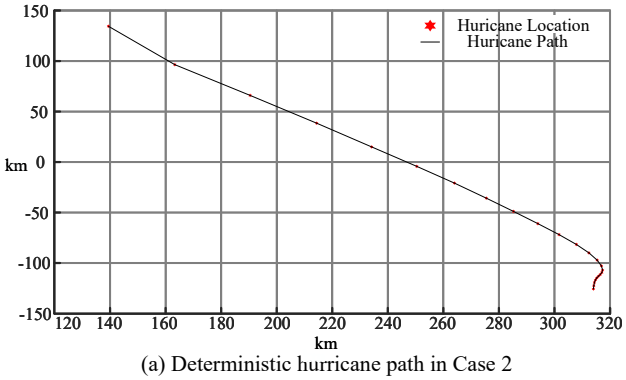

(a) Deterministic hurricane path in Case 2

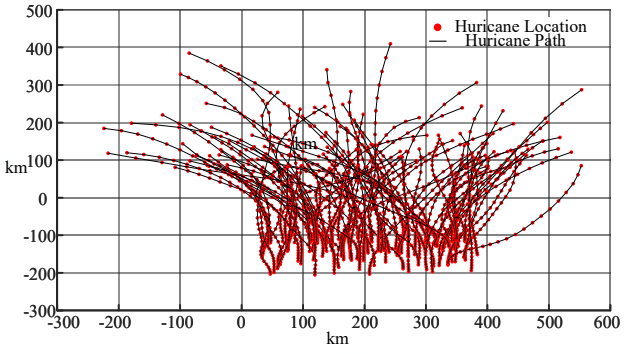

(b) Uncertain hurricane paths in Case 3 and Case 4

Fig. 3. Forecast of hurricane paths.

TABLE II
CASE DESCRIPTION

Case	Design of circumstances	Illustration
Case 1	No hurricane	Analysis of long-term risks of wind power grid-connected systems.
Case 2	Deterministic hurricanen path	Analysis of short-term risk impact of hurricane transit on wind power grid-connected system.
Case 3	Uncertain hurricane Paths	Analysis of the impact of inaccurate hurricane path forecast information on power system risk.
Case 4	Uncertain hurricane paths with no wind farm	Analyze the impact of renewable energy(wind power) on power system risk.

system risks, see Tab II. The forecast of hurricane tracks is shown in Fig. 3.

B. Simulation Results under IEEE RTS-24

The overall load shedding and wind power curtailment for the four case studies are shown in Tab III. The expected load shedding increased from 0.0097 MWh to 40.3539 MWh, then increased to 100.2063 MWh, and finally to 102.4596 MWh. The relative growth percentages were 41501.95%, 148.31%, and 2.24%, respectively. With no hurricane in Case 1, the power line failure depends only on the forced failure probability. Fewer line failures made a lower impact on power outages, and load demands can be satisfied. With a determinate hurricane, the impact of the hurricane on the low latitude power lines at 22:00-24:00 is shown in Fig. 3 (a), and from Fig. 4, the failure probability of power lines 1-3, 1-5, 2-4, 2-6 and 4-9 is 100% in the last two hours, which is also the reason for the sudden increase of expected load shedding, especially in the period of 23:00-24:00 the load shedding of bus 4 exceeds 35 MWh. In Case 3, the hurricane path could not be accurately predicted, and the increase in line failure probability led to more line failures, and the uncertainty of fault combination increased, resulting in the expansion of load shedding in space-time distribution, as shown in Fig. 4 and Fig. 5. In Case 4, with no wind farm under uncertain hurricane, the expected load shedding is improved compared with Case 3, which shows that wind power reduces system risk.

Tab III, Fig. 4 and Fig. 5 can complete the analysis of the deterministic hurricane path. However, the load bus power supply's reliability and system risk level cannot be directly and accurately described for the uncertain hurricane path. The load bus and time slot of maximum load shedding of the four cases are given in Tab III. However, compared with Fig. 5, the load bus with maximum load shedding cannot be determined to have a high-risk level of load shedding. For example, in Case 3, the load shedding time slot of bus 10 is 19:00 to 24:00, but the load shedding time slot of bus 5 starts from 03:00, which means traditional EENS metrics cannot effectively quantify the system risk level.

The DRO-CVaR of load shedding at each load bus is shown in Tab IV. By comparing Tab III, Fig. 4-Fig. 5 and Tab IV, it can be seen that the DRO-CVaR increases numerically and expands in space from Case 1 to Case 4, which is consistent with the analysis results of expected load shedding in Tab

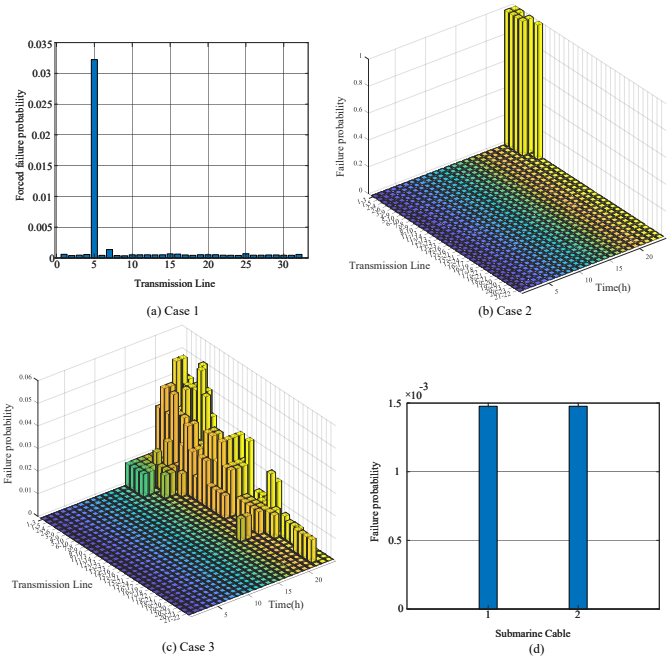

Fig. 4. Failure probability of power transmission lines.

III and Fig. 5. In Case 1, bus 3 has the largest DRO-CVaR, but bus 5 has the maximum load shedding and the total ENNS during horizon. The comparison with Fig. 4(a) can be explained because line 3-9 has the largest forced failure probability. In Case 2, bus 14 has the largest DRO-CVaR. Compared with Fig. 4(a) and Fig. 4(b), it is found that the failure probability of the line connected to bus 14 is lower, which indicates that the small probability event will lead to severe the local load shedding, and the system may have to sacrifice local power demand to meet the power balance so that the system can continue to operate. In Case 3 and Case 4, the spatial distribution of DRO-CVaR of load shedding did not change. Among them, except for bus 5 and bus 14, all other load bus have increased, indicating that system risk increases in the absence of wind power.

The improvement of power system adequacy and reliability by wind power improves not clearly under the uncertain hurricane paths. The DRO-CVaR of wind power curtailment at each wind farm is shown in Tab V. In Case 1, with no hurricane, the DRO-CVaR of wind power curtailment is higher because the wind power is the actual wind farm power output under normal conditions. It can be seen from Tab III that the DRO-CVaR of load shedding at each load bus is very small, and the wind power improves the adequacy and reliability of the system. In Case 2 and Case 3 with the hurricane, as the power output of the wind generator is small or shut down due to the influence of hurricane-induced high wind events, the DRO-CVaR of wind power curtailment in Case 2 is only offshore wind farm 4. In Case 3, the impact of uncertain hurricane path on wind power output is stochastic, and the system is in urgent need of external energy supply to meet

TABLE III
COMPARISON BETWEEN CASE RESULTS

Case	Expected load shedding	Maximum expected load shedding	Power bus of maximum expected load shedding	Time slot of maximum expected load shedding	Wind farm of maximum expected wind power curtailment	Maximum expected wind power curtailment	Time slot of maximum expected wind power curtailment
Case 1	0.097 MWh	0.0118 MWh	Bus 5	20:00-20:59	Off-shore wind farm 4	18.4331 MWh	15:00-15:59
Case 2	40.3539 MWh	35.1188 MWh	Bus 4	22:00-22:59	Off-shore wind farm 4	25.7942 MWh	21:00-21:59
Case 3	100.2063 MWh	5.4832 MWh	Bus 10	23:00-23:59	Off-shore wind farm 4	8.9258 MWh	14:00-14:59
Case 4	102.4596 MWh	5.6266 MWh	Bus 10	23:00-23:59	-	-	-

TABLE IV
DISTRIBUTIONALLY ROBUST CONDITIONAL VALUE AT RISK OF LOAD SHEDDING AT EACH LOAD BUS

Bus	Case 1	Case 2	Case 3	Case 4
1	0	0	0	0
2	0	0	0	0
3	47.2888	90.0877	342.7978	380.8313
4	3.5487	132.1098	243.7633	253.7302
5	31.2889	103.0633	248.9558	245.1449
6	0	143.8844	307.6674	311.7413
7	0	0	0	0
8	0	0	186.1114	194.2259
9	0	0	390.9135	395.6175
10	0	0	435.5894	440.8310
13	0	0	0	0
14	0	258.4053	266.9293	246.3331
15	0	0	0	0
16	0	0	0	0
18	0	0	0	0
19	0	0	89.3267	90.3704
20	0	0	63.0336	63.9083

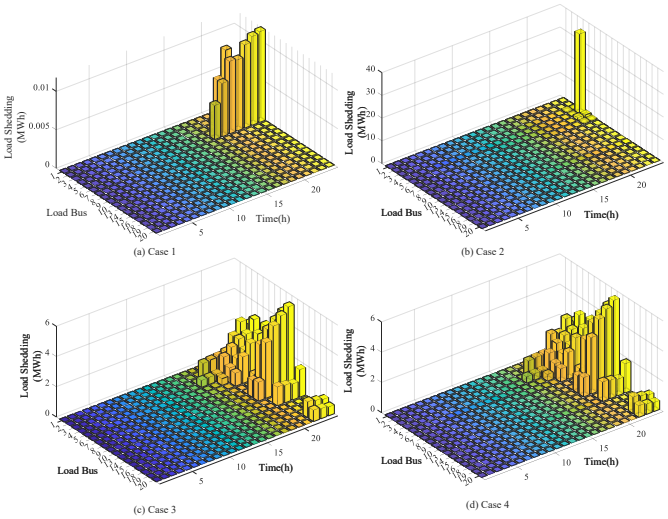

Fig. 5. Expected load shedding at power buses.

the load demand, but the system may not be able to absorb all of wind power in a certain time slot, so the DRO-CVaR of wind power curtailment is between Case 1 and Case 2. Compared with Case 4, it can be seen from Tab III that the DRO-CVaR of load shedding at each load bus is higher without wind power, which indicates that wind power has improved the risk resistance ability of the power systems. Need to pay attention to, the DRO-CVaR of wind power curtailment of offshore wind farms was obviously higher than that of onshore wind farms. This is because the low latitude power lines are

TABLE V
DISTRIBUTIONALLY ROBUST CONDITIONAL VALUE AT RISK OF WIND POWER CURTAILEMNT AT EACH WIND FARM

Wind farm	Grid-connected power bus	Case 1	Case 2	Case 3	Case 4
1	23	5.2236	0	2.7709	0
2	24	81.1963	0	10.9016	0
3	2	1833.9332	0	135.2675	0
4	7	1935.2347	63.9356	165.3553	0

greatly influenced by hurricanes, causing more line failures, and high latitude lines are under the influence of smaller ones. The threat to the line has been reduced as hurricane dispersal process area, less so onshore wind farms wind power curtailment. This also reflects the rationality of wind farm layout and grid-connection power bus selection and suggests active prevention for system operators.

VI. CONCLUSION

In this paper, a distributionally robust resilience assessment model is proposed to quantify the risk level of the power systems with OWFs under uncertain hurricanes. The simulation results show that the time-varying failure probability of overhead lines varies with different hurricane paths, which can better identify the weak points of the power systems. The hurricanes in different places of birth have a greater impact on the power output of OWFs, and the output of OWFs is more volatile than that of onshore wind farms. Besides, the grid-connection of the wind farms during hurricanes improves the system adequacy. The case study verifies that the risk of load shedding increases significantly under uncertain hurricanes, and the nodal reliability of the power supply will be further improved with the help of wind power. The comparison of the results of the four cases proves the effectiveness of the proposed DRO-CVaR as a resilience index, and DRO-CVaR reflects the nodal power supply reliability and system risk level more directly than the expected load shedding. In the future, the hurricane model should be further focused on a region, and the test system will be projected to the coastal areas of China for practical applications.

REFERENCES

[1] S. Najafi Ravadanegh, M. Karimi, and N. Mahdavi Tabatabaei, "Modeling and analysis of resilience for distribution networks," in *Power Systems Resilience*. Springer, 2019, pp. 3–43.

[2] Y. Yang, W. Tang, Y. Liu, Y. Xin, and Q. Wu, "Quantitative resilience assessment for power transmission systems under typhoon weather," *IEEE Access*, vol. 6, pp. 40 747–40 756, 2018.
[3] Y. Meng, M. Matsui, and K. Hibi, "An analytical model for simulation of the wind field in a typhoon boundary layer," *Journal of wind engineering and industrial aerodynamics*, vol. 56, no. 2-3, pp. 291–310, 1995.
[4] H. Zhang, P. Wang, S. Yao, X. Liu, and T. Zhao, "Resilience assessment of interdependent energy systems under hurricanes," *IEEE Transactions on Power Systems*, vol. 35, no. 5, pp. 3682–3694, 2020.
[5] D. Yan and T. Zhang, "Research progress on tropical cyclone parametric wind field models and their application," *Regional Studies in Marine Science*, p. 102207, 2022.
[6] P. N. Georgiou, "Design wind speeds in tropical cyclone-prone regions," 1986.
[7] G. J. Holland, "An analytic model of the wind and pressure profiles in hurricanes," 1980.
[8] R. Schloemer, "Analysis and synthesis of hurricane wind patterns over lake okechobee," *Florida US Weather Bureau, Hydromet. Rep.*, vol. 31, pp. 1–49, 1954.
[9] P. Vickery, P. Skerlj, and L. Twisdale, "Simulation of hurricane risk in the us using empirical track model," *Journal of structural engineering*, vol. 126, no. 10, pp. 1222–1237, 2000.
[10] M. Panteli, C. Pickering, S. Wilkinson, R. Dawson, and P. Mancarella, "Power system resilience to extreme weather: fragility modeling, probabilistic impact assessment, and adaptation measures," *IEEE Transactions on Power Systems*, vol. 32, no. 5, pp. 3747–3757, 2016.
[11] M. Panteli, D. N. Trakas, P. Mancarella, and N. D. Hatziargyriou, "Boosting the power grid resilience to extreme weather events using defensive islanding," *IEEE Transactions on Smart Grid*, vol. 7, no. 6, pp. 2913–2922, 2016.
[12] G. Fu, S. Wilkinson, R. J. Dawson, H. J. Fowler, C. Kilsby, M. Panteli, and P. Mancarella, "Integrated approach to assess the resilience of future electricity infrastructure networks to climate hazards," *IEEE Systems Journal*, vol. 12, no. 4, pp. 3169–3180, 2017.
[13] F. N. I. of Building Sciences), "Multi-hazard loss estimation methodology earthquake model (hazus-mh mr4): Technical manual," 2003.
[14] A. Shafieezadeh, U. P. Onyewuchi, M. M. Begovic, and R. DesRoches, "Age-dependent fragility models of utility wood poles in power distribution networks against extreme wind hazards," *IEEE Transactions on Power Delivery*, vol. 29, no. 1, pp. 131–139, 2013.
[15] H. Macdonald, G. Hawker, and K. Bell, "Analysis of wide-area availability of wind generators during storm events," in *2014 International Conference on Probabilistic Methods Applied to Power Systems (PMAPS)* IEEE, 2014, pp. 1–6.
[16] P. Tavner, *Offshore wind turbines: reliability, availability and maintenance*. IET, 2012, vol. 13.
[17] P. Tavner, R. Gindele, S. Faulstich, B. Hahn, M. Whittle, and D. Greenwood, "Study of effects of weather & location on wind turbine failure rates," in *Proceedings of the European wind energy conference EWEC*, vol. 2010, 2010.
[18] Q. Zhang, X. Wang, W. Du, H. Zhang, and X. Li, "Reliability model of submarine cable based on time-varying failure rate," in *2019 IEEE 8th International Conference on Advanced Power System Automation and Protection (APAP)*. IEEE, 2019, pp. 711–715.
[19] A. Bagheri and C. Zhao, "Distributionally robust reliability assessment for transmission system hardening plan under nk security criterion," *IEEE Transactions on Reliability*, vol. 68, no. 2, pp. 653–662, 2019.
[20] A. Abul'Wafa, A. El'Garably, and S. Nasser, "Power system security assessment under n-1 and n-1-1 contingency conditions," *International Journal of Engineering Research and Technology*, vol. 12, no. 11, pp. 1854–1863, 2019.
[21] I. Dobson, B. Carreras, and D. Newman, "Probabilistic load-dependent cascading failure with limited component interactions," in *2004 IEEE International Symposium on Circuits and Systems (IEEE Cat. No.04CH37512)*, vol. 5, 2004, pp. V–V.
[22] M. Powell, G. Soukup, S. Cocke, S. Gulati, N. Morisseau-Leroy, S. Hamid, N. Dorst, and L. Axe, "State of florida hurricane loss projection model: Atmospheric science component," *Journal of wind engineering and industrial aerodynamics*, vol. 93, no. 8, pp. 651–674, 2005.
[23] P. J. Vickery, "Simple empirical models for estimating the increase in the central pressure of tropical cyclones after landfall along the coastline of the united states," *Journal of applied meteorology*, vol. 44, no. 12, pp. 1807–1826, 2005.
[24] G. J. Holland, "An analytic model of the wind and pressure profiles in hurricanes," 1980.
[25] Q. Zhang, X. Wang, W. Du, H. Zhang, and X. Li, "Reliability model of submarine cable based on time-varying failure rate," in *2019 IEEE 8th International Conference on Advanced Power System Automation and Protection (APAP)*. IEEE, 2019, pp. 711–715.
[26] X. Fu, H.-N. Li, and G. Li, "Fragility analysis and estimation of collapse status for transmission tower subjected to wind and rain loads," *Structural safety*, vol. 58, pp. 1–10, 2016.
[27] M. Ouyang and L. Duenas-Osorio, "Multi-dimensional hurricane resilience assessment of electric power systems," *Structural Safety*, vol. 48, pp. 15–24, 2014.
[28] F. Xiao, J. D. McCalley, Y. Ou, J. Adams, and S. Myers, "Contingency probability estimation using weather and geographical data for on-line security assessment," in *2006 International Conference on Probabilistic Methods Applied to Power Systems*. IEEE, 2006, pp. 1–7.
[29] Y. Liu and C. Singh, "A methodology for evaluation of hurricane impact on composite power system reliability," *IEEE Transactions on Power Systems*, vol. 26, no. 1, pp. 145–152, 2010.
[30] C. Zhao and R. Jiang, "Distributionally robust contingency-constrained unit commitment," *IEEE Transactions on Power Systems*, vol. 33, no. 1, pp. 94–102, 2018.